Photocatalytic carbon dioxide reduction at *p*-type copper(I) iodide

Tomasz Baran,[a][b] Szymon Wojtyła,[a] Angela Dibenedetto,[b][c] Michele Aresta,[c][d] and Wojciech Macyk*[a]

Abstract: A *p*-type semiconductor, CuI, has been synthesized, characterized and tested as a photocatalyst for CO_2 reduction under UV-vis irradiation in presence of isopropanol as hole scavenger. Formation of CO, CH_4 and/or HCOOH was observed. The photocatalytic activity of CuI was attributed to a very low potential of the conduction band edge, amounting ca. –2.28 V vs. NHE. Photocurrents generated by the studied material confirm a high efficiency of the photoinduced interfacial electron transfer processes. Our studies show that *p*-type semiconductors may be effective photocatalysts for CO_2 reduction, even better than extensively studied *n*-type titanium dioxide, due to the low potential of the conduction band edges.

Introduction

Photocatalytic carbon dioxide reduction is a challenging process in which, similarly to photosynthesis, solar light can be converted into chemical energy. This reaction is, thus, the opposite of most commonly studied photocatalytic reactions in which pollutants are photooxidized to CO_2 and, obviously, the energetics is different. Nevertheless, the same photocatalysts (mainly TiO_2) are usually tested in both cases. Most of metal oxides, being *n*-type semiconductors, offer high oxidation properties upon excitation, but at the same time they are relatively mild reductants. In this paper we propose an alternative approach to photocatalytic CO_2 reduction, based on the use of *p*-type semiconductors, which in general disclose better reducing- and worse oxidation-properties in comparison to *n*-semiconductors.

Solar energy driven photofixation and photoreduction of carbon dioxide is a prospective application of semiconductor-based photocatalysis. Photocatalytic processes have been intensively studied for water and air purification, photodynamic processes in medicine, as well as for water splitting.[1–3] Shrinking resources of fossil fuels and an increasing CO_2 level in the atmosphere, motivate scientists to consider photocatalysis as a potential method enabling CO_2 utilization.[4–7] Until now numerous materials were tested as photocatalysts for CO_2 reduction, including: TiO_2, CdS, ZnO, ZnS, Cu_2O, WO_3, $BiVO_4$, Ta_2O_5, and SiC, as well as hybrid systems involving co-catalysts.[8–14]

[a] Prof. W. Macyk, Dr. T. Baran, MSc. S. Wojtyła
Faculty of Chemistry, Jagiellonian University
Ingardena 3, 30-060 Kraków, Poland
e-mail: macyk@chemia.uj.edu.pl
[b] Prof. A. Dibenedetto, T. Baran
Department of Chemistry, University of Bari
Orabona, 4, 70125 Bari, Italy
[c] Prof. M. Aresta, Prof. A. Dibenedetto
CIRCC, Via Celso Ulpiani, 27, 70126 Bari,
[d] IC2R srl, Technopolis, via Casamassima km 3, Valenzano, Bari 70100, Italy.
* Corresponding author e-mail: Tel: +48 12 663 2222; e-mail: macyk@chemia.uj.edu.pl (Wojciech Macyk)

The photocatalytic reduction of CO_2 may afford a variety of products, depending on the photocatalyst, solvent and electron donor.[15–17] Unlike one-electron reduction of CO_2 to $CO_2^{\bullet-}$, a proton-assisted multi-electron reduction of carbon dioxide requires a lower energy (less negative potentials) and leads to stable products. The final oxidation state of carbon depends on the number of transferred electrons. Standard redox potentials of CO_2 reduction in water vary from –0.61 V for CO_2/HCOOH ($2e^-$ reduction) to –0.24 V for CO_2/CH_4 ($8e^-$ reduction).[18]

It is worth to recall that semiconductors may be categorized as intrinsic, *p*- and *n*-type semiconductors.[19] An intrinsic material is a perfect crystalline semiconductor, while *n*- and *p*-type materials contain impurities or dopants in their lattices, having an electron acceptor or donor character, respectively. Since the interfacial electron transfer is a critical step in photocatalytic processes and the excess of electrons leads to photodegradation of photocatalyst, *p*-type semiconductors, in which holes are majority charges, seem to be more resistant to photocorrosion than *n*-type.[20–22] In fact, the *p*-type semiconductors have in general lower Fermi levels than *n*-type materials, therefore they are more resistant to oxidation than *n*-type semiconductors.

Copper(I) iodide is a direct semiconductor with a zinc-blende structure below 643 K (γ-CuI), a wurtzite structure between 643 and 673 K (β-CuI) and a rock salt structure above 673 K (α-CuI).[23] The low temperature γ-phase is a wide-bandgap semiconductor with the bandgap energy close to 3.1 eV and the potential of conduction band edge of *ca.* –2.1 V *vs.* SHE (calculated from data reported elsewhere).[24,25] The valence band is constituted of Cu-*d* and I-*p* orbitals.[23,26] γ-CuI is a *p*-type semiconductor, while β- and particularly α-phases show the character of an ionic conductor.

Recent studies show that copper(I) iodide is a promising material for application in organic electronic devices. CuI characterized by a high conductivity exhibits a high optical transparency in visible light. These properties make CuI thin films very useful in dye sensitized solar cell,[27] or as hole-injection layers in OLED.[28] The γ-phase copper(I) iodide can also find application in bipolar diodes (*e.g. p*-CuI/*n*-ZnO)[29] or as an electrocatalyst.[30] However, the activity of CuI in photocatalytic processes remains unraveled. To our best knowledge there are no reports on application of copper(I) iodide as a photocatalyst. Very recently, CuI–RGO (reduced graphene oxide) system was tested in photocatalytic degradation of organic dyes, however, in these studies copper(I) iodide did not play the role of a photocatalyst (did not absorb light) but it was used as a core in the core-shell structure of CuI-RGO.[31]

In our recent papers on carbon dioxide utilization we described semiconductor systems capable of one-[32,33] and multi-electron reduction of CO_2,[14] as well as a hybrid, photocatalytic-enzymatic reduction of CO_2 to methanol.[34,35] The use of *p*-type photocatalysts for carbon dioxide reduction can be justified by considerably low potentials of conduction band edges offering significantly better reduction properties compared to those characteristic for a majority of *n*-type materials. Thus,

here we report the first evidence of photocatalytic activity of CuI and the first studies on the application of this material for photocatalytic reduction of CO_2.

Results and Discussion

The commercial CuI powder is composed of particles in a random size range of several tens of micrometers, as shown in the SEM image in Fig. 1a. When water was quickly injected into the CuI acetonitrile solution, a white precipitate was instantly formed due to the strong antisolvent effect of water. Recrystallized CuI forms irregular aggregates of 50-300 nm (Fig. 1b).

The crystal structure of recrystallized copper(I) iodide was determined by X-ray diffraction (XRD, Fig. 2). The main phase of the as-prepared material is γ-CuI with the diffraction peaks at 25, 29, 43, 50, 52, 62, 67 and 69°, attributed to (111), (200), (220), (311), (222), (400), (331) and (420) planes, respectively (JCPDS, No. 06-0246). The structure of γ-CuI was refined in the F4-3m space group. Particle sizes calculated from Scherrer equation are 60 and 20 nm for commercial and recrystallized CuI, respectively.

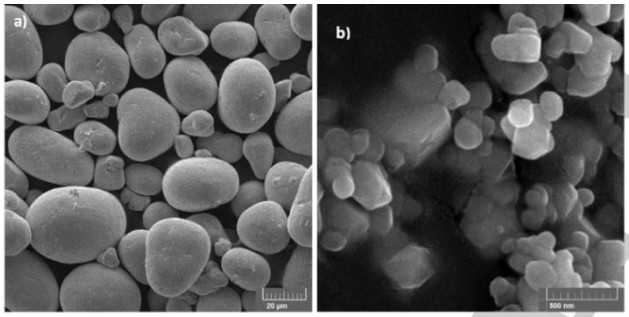

Figure 1. SEM images of commercial (a) and recrystallized (b) copper(I) iodide.

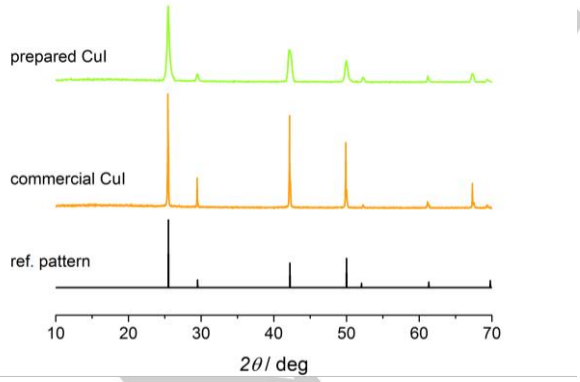

Figure 2. XRD pattern of the recrystallized CuI material (green), commercial copper iodide (orange line) and the reference pattern of γ-CuI – JCPDS card no. 06-0246 (black).

Diffuse reflectance spectra of the prepared copper(I) iodide, converted to Kubelka-Munk function, are presented in Fig. 3. Copper(I) iodide shows absorption of light of wavelength lower than 420 nm. The band gap energy was estimated from Tauc's plot, $[KM \cdot E]^n$ vs. E, where E – photon energy, KM – Kubelka-Munk function, the n index is equal to 2 for direct allowed transition. The calculated band gap energy, E_{BG}, for the direct semiconductor is equal to 3.30 eV. The value of E_{BG} of commercial copper(I) iodide was 3.15 eV, as measured for the material obtained from Sigma Aldrich.

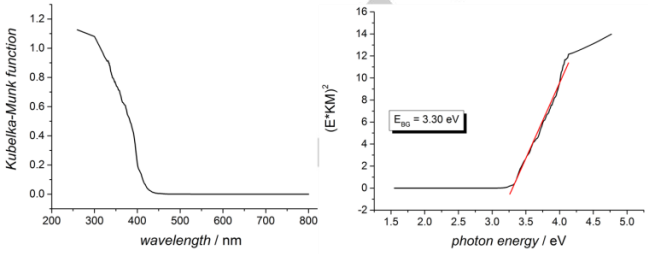

Figure 3. Transformed diffuse reflectance spectrum of recrystallized CuI (left) and estimation of its band gap energy (right).

The photoactivity of CuI was analyzed by photocurrent measurements in the potential range of 0.65 to 0.15 V *vs.* RHE (at pH = 6.9, irradiation at 390 nm; Fig. 4). Only cathodic photocurrents, typical for *p*-type semiconductors, were generated under the applied conditions. Under nitrogen atmosphere the photocurrent density varied from a few up to 70 μA cm^{-2}. In the presence of CO_2 a significant increase of the photocurrent density was observed (up to 200 μA cm^{-2}). Under oxygen-free atmosphere the cathodic photocurrent results from two parallel processes: water splitting and CO_2 reduction. Since pH was kept at the same level in both measurements the photocurrent amplification under CO_2 atmosphere can be attributed to the reduction of carbon dioxide. Prolonged photocurrent measurements under chopped light prove the stability of recrystallized CuI up to more than 5 hours (see Fig. S1; SI).

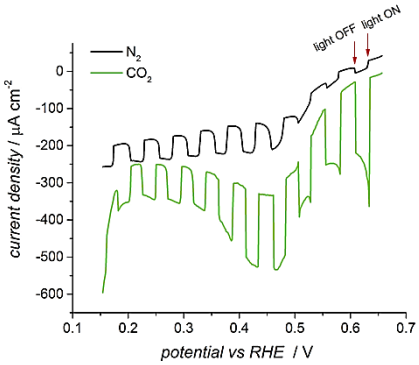

Figure 4. Photocurrents recorded for CuI as a function of the applied potential. Measurements with chopped incident light (390 nm). The electrolyte (pH = 6.9) was saturated with nitrogen or carbon dioxide.

Mott-Schottky measurements (electrochemical impedance spectroscopy) were employed to determine the flat band potential of the photocatalyst. The capacitance of

the space charge layer depends on the applied potential according to the formula:

$$\frac{1}{C_{SC}^2} = \frac{2}{e\varepsilon\varepsilon_0 N}\left(E - E_{FB} - \frac{kt}{e}\right),$$

where ε is the dielectric constant of the sample, ε_0 is the vacuum permittivity, e is the charge of electron, N is the concentration of hole acceptor (for *p*-type semiconductors), E is the applied potential, E_{FB} is the flat band potential, k is the Boltzmann constant, T denotes the temperature and C (or *CPE*) is the capacitance of the space charge layer.[36] The impedance Z_{CPE} of the *CPE* is given by:

$$Z_{CPE} = \frac{1}{Q(j\omega)^{\alpha}}$$

where ω is the frequency and α equals unity for an ideal capacitor. Figure 5 shows the electrochemical impedance spectra (Nyquist plots) measured at various potentials in the range of 0 to 0.6 V in the dark. Data shown in Fig. 5 are fitted considering the equivalent circuit depicted in the inset (*R1* and *R3* mean solution and polarization resistances, respectively, *CPE* is a constant phase element).

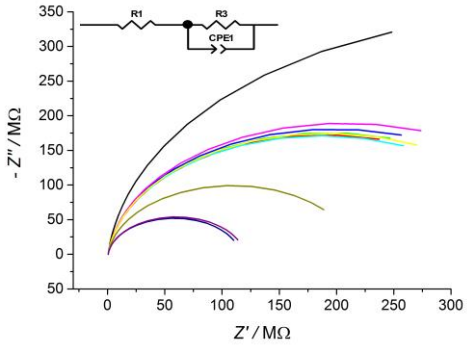

Figure 5. Nyquist plots measured in the dark at various potential in the range of 0 to 0.6 V *vs.* SCE. The inset presents the equivalent circuit used to fit the impedance data.

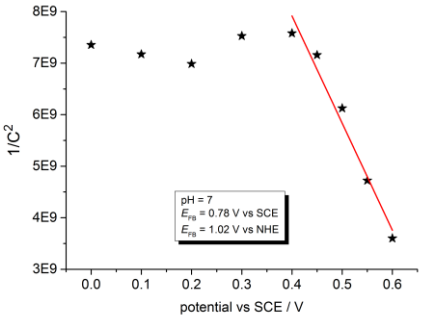

Figure 6. Mott-Schottky plot for CuI. E_{FB} was calculated from the linear fitting (red curve; $y = -2.08 \cdot 10^{10} x + 1.62 \cdot 10^{10}$).

Resulting Mott-Schottky plot (dependence of the calculated capacitance on the electrode potential) is shown in Fig. 6. The negative slope of the plot proves the *p*-type nature of the recrystallized CuI photocatalyst. The flat band potential is close to the potential of the upper edge of valence band for *p*-type semiconductors[37] and is equal to 0.78 V *vs.* SCE (1.02 V *vs.* NHE). Knowing the flat band potential and E_{BG} (3.30 eV, *vide supra*), we can estimate the potential of the conduction band edge, E_{CB}, which amounts to –2.28 V *vs.* NHE. It is sufficiently negative to reduce CO_2 (redox potentials of CO_2 reduction vary from –1.9 V *vs.* NHE for $CO_2/CO_2^{\bullet-}$ to –0.24 V *vs.* NHE for CO_2/CH_4 (values for aqueous solutions, pH = 7).[18]

The photocatalytic reduction of carbon dioxide in the presence of the recrystallized CuI has been tested. Irradiation of the suspensions of CuI in chloroform in the presence of isopropanol as H-transfer agent resulted in the reduction of CO_2 to various products, including formic acid, carbon monoxide and methane, as summarized in Fig. 7, Table 1. Chloroform has been selected in order to facilitate analysis of products (GC, NMR). Formic acid was determined by ^{1}H-NMR (Fig. 7a) while gaseous products (carbon monoxide, methane) were quantified basing on GC analysis (Fig. 7b). The commercial sample of copper(I) iodide (Sigma-Aldrich) was able to only reduce CO_2 to CO under the same reaction conditions. After 5-hours irradiation the concentration of carbon monoxide in the gas phase above the reaction mixture reached 160 μmol dm^{-3} (the headspace volume was 9.5 mL). The use of recrystallized CuI led to generation of the enhanced amounts of the reduction products (formic acid, carbon monoxide and methane; Fig. 8). The formation rates of all products were higher than those recorded for commercial CuI. For instance, after 5 hours of irradiation formic acid was found as the main product in solution, with a concentration exceeding 800 μmol dm^{-3}. A commercial TiO_2 photocatalyst (P25; *n*-type material) applied under identical conditions showed very low photocatalytic activity – 5-hours irradiation resulted in production of 3 μmol dm^{-3} of CH_4 and 2.7 μmol dm^{-3} of H_2 (Fig. 7). Neither CO nor HCOOH was detected after irradiation.

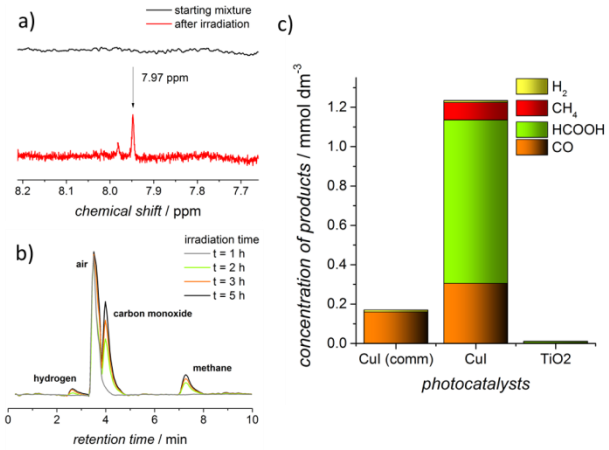

Figure 7. Products of carbon dioxide reduction in the presence of various photocatalysts and isopropanol as the electron donor: a) ^{1}H-NMR spectra of the reaction mixture before and just after irradiation in the presence of CuI (spectra recorded after addition of CD_3Cl); b) GC analysis of gas phase above the reaction mixture (photocatalyst: CuI); c) summarized results of products analysis after 5-hours irradiation.

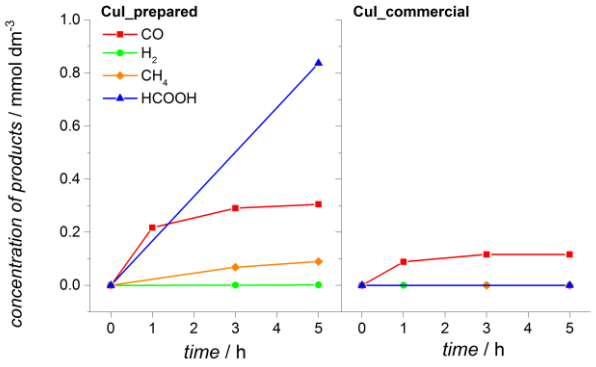

Figure 8. Photoreduction of CO_2 in the presence of recrystallized (left) and commercial (right) CuI.

Table 1. Comparison of activity of various photocatalyts toward CO_2 reduction to selected products. Concentrations of all products in mmol dm^{-3}. Reaction conditions: solvent - deoxygenated chloroform + isopropanol 10 %vol. Irradiation for 5 h by 150 W XBO arc lamp (λ > 300 nm)

	CuI commercial	CuI recrystallized	TiO_2, P25
CO	160	300	-
H_2	-	11	2.7
CH_4	-	114	3.0
HCOOH	2.2	813	-

In order to exclude the possibility of other routes of C_1 products formation (*e.g.* oxidation of contaminants originating from an incomplete removal of organic solvents during preparation of the photocatalyst or oxidation of isopropanol) additional control experiments were performed. The suspensions of photocatalysts were irradiated in the absence of CO_2 (solutions were purged with argon in order to remove CO_2 and O_2 dissolved in chloroform) and the presence of isopropanol. Neither CH_4 nor CO and any other carbon-containing products were detected (data not shown), indicating that all observed products originate from the reduction of carbon dioxide and not from the oxidation of any organic component of the system. The reduction did not proceed in systems lacking one of the following components: the photocatalyst, light, electron donor or carbon dioxide (tested in the systems with recrystallized and commercial CuI, data not shown). These experiments prove, that isopropanol acted as the hole scavenger giving rise to acetone production, a typical product of *i*-PrOH oxidation, confirmed also by ^{13}C-NMR analysis, peaks 29.6 and 206 ppm shown in Fig. S2 in Supporting Information. Moreover, further oxidation of acetone cannot be excluded, since its oxidation potential is 0.126 V.[38] In order to understand better the stability of the material, XRD pattern of CuI used previously as a photocatalyst for 5 hours has been collected. Results (compare Fig. S3; SI) prove that the material after 5 h of irradiation is composed mainly of copper iodide, however, some peaks characteristic for metallic copper, copper(I) oxide and copper(II) oxide have been found on the diffractogram.

Conclusions

Prepared *p*-type copper iodide was successfully applied as a photocatalyst for carbon dioxide reduction. Recrystallization of copper iodide leads to the formation of significantly smaller, more photoactive particles. Small size of particles reflects in: i) a larger specific surface area; ii) more efficient transport of photogenerated charges from the bulk to the surface; iii) a higher rate of carbon dioxide photoreduction due to increased amount of adsorbed CO_2.

The analysis of photocurrents generated by the studied material confirms a high efficiency of the photoinduced interfacial electron transfer processes for CuI. This effect may result either from a good charge separation or from a less efficient recombination.

The mechanism of photocatalytic process is shown in Fig. 9. Potentials of the conduction band edges of *p*-type semiconductors are usually lower than those of *n*-type materials (–2.28 V *vs.* NHE for CuI estimated from the Mott-Schottky analysis, compared to *ca.* –1.0 V *vs.* NHE for P25 TiO_2 measured using spectroelectrochemical method[39]). Reduction of carbon dioxide requires good reduction properties (*e.g.* –1.8 V for one-electron reduction to $CO_2^{\bullet-}$ or –0.61 to –0.24 V for multi-electron processes leading to the formation of formic acid or methane, respectively). Therefore the photocatalytic CO_2 reduction should be thermodynamically favored in the presence of *p*-type semiconductors characterized by low potentials of conduction band edges. In the case of *p*-type materials photocorrosion leads to the formation of metal(0).[40] This process may, to some extent, have a positive influence on the CO_2 reduction efficiency, as the metallic nanoparticles may act as co-catalysts (*e.g.* electron sinks), however, this effect requires a deeper study. Stability and photostability of semiconductors, both *n*- and *p*-type, depends in general on the redox properties of the system components (in particular of the applied solvent),[41] therefore it can be controlled, at least to some extent. This opens a possibility to further improvement of (photo)stability of the photocatalyst. Our studies show that *p*-type CuI may appear an effective photocatalyst of CO_2 reduction. Very likely *p*-type semiconductors may often appear better photocatalysts of this reaction than extensively studied *n*-type titanium dioxide.[42,43] Other solvents will be considered in further studies focused on the process optimization and scaling up.

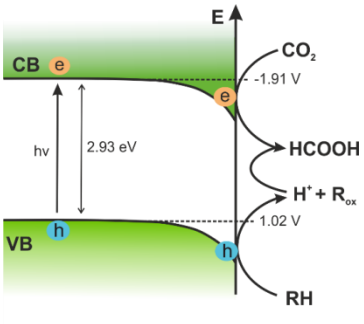

Figure 9. Mechanism of CO_2 reduction on the *p*-type semiconductors.

Experimental Section

Nanocrystalline copper(I) iodide has been prepared according to the method described elsewhere with minor modifications.[44] 0.1 g of commercial CuI powder (Sigma Aldrich) was dissolved in 3 ml of acetonitrile by ultrasonication. 15 mL of water was quickly injected into the CuI solution through a syringe pinhole under vigorous magnetic stirring. Formed white precipitate was collected by centrifugation, washed with water (3 times) and ethanol (once) and dried in air at 80°C for 12 hours.

UV-Vis diffuse reflectance spectra of CuI were recorded using a UV-3600 spectrophotometer (*Shimadzu*) equipped with an integrating sphere (15 cm dia.). The sample was ground with $BaSO_4$ (1:50 wt. ratio). The prepared material was analyzed using the X-ray powder diffractometer (MiniFlex 600, *Rigaku*) operated at 40 kV. Data were collected in the angular range of $20°<2\Theta<70°$ for a total counting time of 45 min/pattern. SEM images were collected at the scanning electron microscope (Vega 3 LMU, *Tescan*) equipped with an LaB_6 cathode. A three-electrode set-up was employed for photocurrent measurements. The electrolyte solution was composed of 0.1 mol dm^{-3} potassium hydrogen phthalate (pH = 4.1). Electrolyte was saturated by N_2 or CO_2 before each scan. Platinum and saturated calomel electrode were used as counter and reference electrodes, respectively. The working electrodes were prepared by covering the FTO glass with a photocatalyst suspension. A LED illuminator (λ = 390 nm) was used for irradiation. The working electrodes were irradiated from the backside, through the FTO, in order to minimize the influence of the thickness of the semiconductor layer on the photocurrent. The electrochemical measurements were controlled by the electrochemical analyzer (PGSTAT 302N, Autolab). Electrochemical impedance measurements were performed in deoxygenated 0.1 mol dm^{-3} K_2HPO_4 + KH_2PO_4 electrolyte solution, pH = 7.1. Impedance spectra were recorded at fixed potentials in the frequency range 1 MHz to 0.1 Hz using Autolab PGSTAT 302N analyzer. The potential was stepped by 50 mV in the range from 0 to 0.6 V *vs*. SCE with a waiting time of 180 s before the next spectra were recorded. The impedance data were fitted using equivalent circuits.

Photocatalytic tests of CO_2 reduction were performed in a quartz cylindrical cuvette (total volume of 15 mL) equipped with a rubber septum. The photocatalyst (1 g dm^{-3}) was suspended in distilled, deoxygenated chloroform (5 mL). Isopropanol was used as an electron and proton donor (0.5 mL). Noteworthy, isopropanol is used in industry as an H_2-transfer agent. The suspension was purged with CO_2 for 15 minutes in an ice bath. The suspension was irradiated in the sealed cuvette using a 150 W XBO arc lamp as a light source (λ > 300 nm). Gas samples were collected at fixed time intervals during irradiation and analyzed by GC (*Thermo Scientific* Focus GC with a TCD detector and Carboxen-1000 plot column). Liquid samples were filtered through syringe filters (0.2 µm) diluted 1:1 with CD_3Cl and analyzed with NMR (*Bruker* 600 MHz).

Acknowledgements

The authors thank MSc. Anna Regiel-Futyra for SEM measurements. The support from the Foundation for Polish Science within the VENTURES/2011-8/1 Project and the Project TEAM/2012-9/4, both co-financed by the EU European Regional Development Fund, is highly acknowledged. Collaboration with IC^2R srl and VALBIOR-Apulia Network is acknowledged.

Keywords: photocatalysis • CO_2 reduction • *p*-type semiconductors • copper(I) iodide

[1] S. Füldner, R. Mild, H. I. Siegmund, J. A. Schroeder, M. Gruber, B. König, *Green Chem.* **2010**, *12*, 400–406.
[2] T. Baran, W. Macyk, *J. Photochem. Photobiol. Chem.* **2012**, *241*, 8–12.
[3] K. Szaciłowski, W. Macyk, A. Drzewiecka-Matuszek, M. Brindell, G. Stochel, *Chem. Rev.* **2005**, *105*, 2647–2694.
[4] M. Mikkelsen, M. Jørgensen, F. C. Krebs, *Energy Environ. Sci.* **2010**, *3*, 43–81.
[5] K. Kočí, L. Obalová, Z. Lacný, *Chem. Pap.* **2008**, *62*, 1–9.
[6] J. Albo, M. Alvarez-Guerra, P. Castaño, A. Irabien, *Green Chem.* **2015**, *17*, 2304–2324.
[7] M. Aresta, A. Dibenedetto, A. Angelini, *Chem. Rev.* **2014**, *114*, 1709–1742.
[8] K. Kočí, L. Matějová, M. Reli, L. Čapek, V. Matějka, Z. Lacný, P. Kustrowski, L. Obalová, *Catal. Today* **2014**, *230*, 20–26.
[9] M. Anpo, *J. CO2 Util.* **2013**, *1*, 8–17.
[10] S. Wang, X. Wang, *Appl. Catal. B Environ.* **2015**, *162*, 494–500.
[11] T. Ohno, N. Murakami, T. Koyanagi, Y. Yang, *J. CO2 Util.* **2014**, *6*, 17–25.
[12] P. Pathak, M. J. Meziani, L. Castillo, Y.-P. Sun, *Green Chem.* **2005**, *7*, 667–670.
[13] A. Dhakshinamoorthy, S. Navalon, A. Corma, H. Garcia, *Energy Environ. Sci.* **2012**, *5*, 9217–9233.
[14] T. Baran, S. Wojtyła, A. Dibenedetto, M. Aresta, W. Macyk, *Appl. Catal. B Environ.* **2015**, *178*, 170–176.
[15] B.-J. Liu, T. Torimoto, H. Matsumoto, H. Yoneyama, *J. Photochem. Photobiol. Chem.* **1997**, *108*, 187–192.
[16] S. N. Habisreutinger, L. Schmidt-Mende, J. K. Stolarczyk, *Angew. Chem. Int. Ed.* **2013**, *52*, 7372–7408.
[17] M. Aresta, A. Dibenedetto, A. Angelini, *Philos. Trans. R. Soc. Math. Phys. Eng. Sci.* **2013**, *371*, 20120111.
[18] E. Fujita, *Coord. Chem. Rev.* **1999**, *185–186*, 373–384.
[19] A. Hernández-Ramírez, I. Medina-Ramirez, in *Photocatalytic Semicond.*, Springer International Publishing, Cham, **2015**.
[20] H. Gerischer, M. Lübke, *Berichte Bunsenges. Für Phys. Chem.* **1983**, *87*, 123–128.
[21] C. A. Mead, W. G. Spitzer, *Phys. Rev. Lett.* **1963**, *10*, 471–472.
[22] M. Grätzel, *Nature* **2001**, *414*, 338–344.
[23] M. Grundmann, F.-L. Schein, M. Lorenz, T. Böntgen, J. Lenzner, H. von Wenckstern, *Phys. Status Solidi A* **2013**, *210*, 1671–1703.
[24] V. P. S. Perera, K. Tennakone, *Sol. Energy Mater. Sol. Cells* **2003**, *79*, 249–255.
[25] K. Tennakone, G. R. R. A. Kumara, I. R. M. Kottegoda, V. P. S. Perera, P. S. R. S. Weerasundara, *J. Photochem. Photobiol. Chem.* **1998**, *117*, 137–142.
[26] K.-S. Song, *J. Phys. Chem. Solids* **1967**, *28*, 2003–2009.
[27] A. R. Zainun, M. H. Mamat, U. M. Noor, M. Mohammad Rusop, *Adv. Mater. Res.* **2013**, *667*, 447–451.
[28] P. Stakhira, V. Cherpak, D. Volynyuk, F. Ivastchyshyn, Z. Hotra, V. Tataryn, G. Luka, *Thin Solid Films* **2010**, *518*, 7016–7018.
[29] F.-L. Schein, H. von Wenckstern, M. Grundmann, *Appl. Phys. Lett.* **2013**, *102*, 092109.
[30] G. Karim-Nezhad, N. Alipour, *Curr. Chem. Lett.* **2014**, *3*, 133–140.
[31] J. Choi, D. A. Reddy, M. J. Islam, B. Seo, S. H. Joo, T. K. Kim, *Appl. Surf. Sci.* **n.d.**, DOI 10.1016/j.apsusc.2015.07.170.
[32] M. Aresta, A. Dibenedetto, T. Baran, S. Wojtyła, W. Macyk, *Faraday Discuss.* **2015**, *183*, 413–427.
[33] T. Baran, A. Dibenedetto, M. Aresta, K. Kruczała, W. Macyk, *ChemPlusChem* **2014**, *79*, 708–715.
[34] A. Dibenedetto, P. Stufano, W. Macyk, T. Baran, C. Fragale, M. Costa, M. Aresta, *ChemSusChem* **2012**, *5*, 373–378.
[35] M. Aresta, A. Dibenedetto, T. Baran, A. Angelini, P. Łabuz, W. Macyk, *Beilstein J. Org. Chem.* **2014**, *10*, 2556–2565.
[36] S. P. Harrington, T. M. Devine, *J. Electrochem. Soc.* **2009**, *156*, C154–C159.
[37] Y. Nakabayashi, M. Nishikawa, Y. Nosaka, *Electrochimica Acta* **2014**, *125*, 191–198.
[38] H. Adkins, R. M. Elofson, A. G. Rossow, C. C. Robinson, *J. Am. Chem. Soc.* **1949**, *71*, 3622–3629.
[39] M. Bledowski, L. Wang, A. Ramakrishnan, O. V. Khavryuchenko, V. D. Khavryuchenko, P. C. Ricci, J. Strunk, T. Cremer, C. Kolbeck, R. Beranek, *Phys. Chem. Chem. Phys.* **2011**, *13*, 21511–21519.
[40] R. van de Krol, in *Photoelectrochem. Hydrog. Prod.* (Eds.: R. van de Krol, M. Grätzel), Springer US, **2012**, pp. 13–67.
[41] H. Gerischer, *J. Vac. Sci. Technol.* **1978**, *15*, 1422–1428.
[42] B. Michalkiewicz, J. Majewska, G. Kądziołka, K. Bubacz, S. Mozia, A. W. Morawski, *J. CO2 Util.* **2014**, *5*, 47–52.
[43] J. Fu, S. Cao, J. Yu, J. Low, Y. Lei, *Dalton Trans.* **2014**, *43*, 9158.
[44] R. Kozhummal, Y. Yang, F. Güder, U. M. Küçükbayrak, M. Zacharias, *ACS Nano* **2013**, *7*, 2820–2828.

Entry for the Table of Contents

FULL PAPER

Copper(I) iodide, a *p*-type semiconductor, shows a significantly higher photoactivity toward CO_2 reduction than extensively studied *n*-type titanium dioxide.

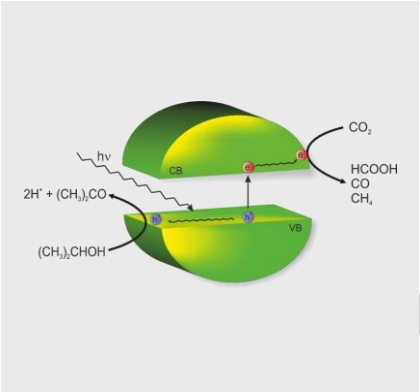

*Tomasz Baran, Szymon Wojtyła, Angela Dibenedetto, Michele Aresta and Wojciech Macyk**

Page No. – Page No.

Photocatalytic carbon dioxide reduction at *p*-type copper(I) iodide